The pasta phase and its consequences on neutrino opacities

M. D. Alloy[1,*] and D. P. Menezes[2,†]

[1] *Universidade Federal da Fronteira Sul, Chapecó, SC, CEP 89.812-000, Brazil.*
[2] *Depto de Física CFM, Universidade Federal de Santa Catarina, Florianópolis, SC CP.476, CEP 88.040-900, Brazil*

(Dated: 4 de novembro de 2010)

In this paper, we calculate the diffusion coefficients that are related to the neutrino opacities considering the formation of nuclear pasta and homogeneous matter at low densities. Our results show that the mean free paths are significantly altered by the presence of nuclear pasta in stellar matter when compared with the results obtained with homogeneous matter. These differences in neutrino opacities certainly influence the Kelvin-Helmholtz phase of protoneutron stars and consequently the results of supernova explosion simulations.

I. INTRODUCTION

When massive stars ($8\ M_\odot < M < 30\ M_\odot$) exhausts its fuel supply, the forces that support the stars core quickly retreat, and the core is almost instantly crushed by gravity, which triggers a type II supernova explosion. The remnant of the gravitational collapse of the core of a massive star is a compact star or a black hole, depending on the initial condition of the collapse. Newly-born protoneutron stars (PNS) are hot and rich in leptons, mostly e^- and ν_e and have masses of the order of $1-2\ M_\odot$ [1, 2]. During the very beginning of the evolution, most of the binding energy, of the order of 10^{53} ergs is radiated away by the neutrinos.

The composition of protoneutron and neutron stars remains a source of intense speculation in the literature. Whether their internal structure is formed by nucleons and leptons, by other light baryons and leptons, by baryons, leptons and quarks (bearing or not a mixed phase), by baryons, leptons and kaons or by other possible composition, is still unknown. The neutrino-signals detected by astronomers can be used as a constraint to infer protoneutron star composition [2, 3]. For the same purpose, theoretical studies involving different possible equations of state obtained for all sorts of matter composition have to be done because the temporal evolution of the PNS in the so-called Kelvin-Helmholtz epoch, during which the remnant compact object changes from a hot and lepton-rich PNS to a cold and deleptonized neutron star depends on two key ingredients: the equation of state (EoS) and its associated neutrino opacity at supranuclear densities [3, 4].

Neutrinos already present or generated in the PNS hot matter escape by diffusion (not free streaming) because of the very high densities and temperatures involved. The neutrino opacity is calculated from the scattering and absorption reactions that take place in the medium and hence, related to its mean free path, which is of the order of 10 cm and much smaller than the protoneutron star radius [5]. In the diffusion approximation used to obtain the temporal evolution of the PNS in the Kelvin-Helmholtz phase, the total neutrino mean free path depends on the calculation of diffusion coefficients, which, in turn, depend on the chosen EoS. At zero temperature no trapped neutrinos are left in the star because their mean free path would be larger than the compact star radius.

A complete equation of state capable of describing matter ranging from very low densities to few times saturation density and from zero temperature to around 50 MeV is a necessary step towards the understanding of PNS evolution. The constitution of the PNS crust plays a definite role in the emission of neutrinos. For this reason, the pasta phase, present in very low nuclear matter as the crust of PNS are included in the investigation of the neutrino opacity in the present work.

A few words on the pasta phase follow. It is a frustrated system [6–10] present at densities of the order of 0.006 - 0.1 fm^{-3} [11] in neutral nuclear matter and 0.029 - 0.065 fm^{-3} [12, 13] in β-equilibrium stellar matter, where a competition between the strong and the electromagnetic interactions takes place. The basic shapes of these complex structures were named [6] after well known types of cheese and pasta: droplets = meat balls (bubbles = Swiss cheese), rods = spaghetti (tubes = penne) and slabs = lasagna, for three, two and one dimensions respectively. The pasta phase is the ground state configuration if its free energy per particle is lower than the corresponding to the homogeneous phase at the same density.

The evolution of PNS and simulation of supernova explosion have already been considered for different matter compositions, some with the inclusion of the pasta phase [3, 4, 7, 14, 15]. From [3, 4] one can see that the transport properties are significantly affected by the presence or absence of hyperons and of the mixed phase in hybrid stars. In [7] the linear response of the nuclear pasta to neutrinos was calculated with a semi-classical simulation and the muon and taon neutrinos mean-free path were described by the static structure factor of the pasta evaluated with Metropolis Monte Carlo simulations. In [14] rod-like (two dimensions) and slab-like (one dimension) pasta structures were included in the calculation

* E-mail me at:alloy@uffs.edu.br
† E-mail me at:debora@fsc.ufsc.br

of neutrino opacity within quantum molecular dynamics. A very interesting conclusion was that the pasta phase occupies 10-20% of the mass of the supernova core in the later stage of the collapse.

In the present work we investigate the influence of the pasta phase on the neutrino opacity by showing the effects on the diffusion coefficients. The pasta phase is calculated with the coexistence phases method (CP) in a mean field approximation [11, 13, 16]. We consider only nucleons and leptons in the EoS in β-equilibrium. In the pasta structure only electron neutrinos are considered.

In section II we present the formalism used to obtain the equation of state, in section III the recipe used for the construction of the pasta phase is outlined, in section IV the expressions used to calculate the neutrino cross sections and related mean free path are given and in section V our results are shown and the main conclusions are discussed.

II. FORMALISM

We consider a system of protons and neutrons with mass M interacting with and through an isoscalar-scalar field ϕ with mass m_s, an isoscalar-vector field V^μ with mass m_v and an isovector-vector field $\mathbf{b}_\mu$ with mass m_ρ described by the well known non-linear Walecka model (NLWM) [17]. We impose β-equilibrium and charge neutrality with neutrino trapping at finite temperature. At zero temperature no neutrinos are left in the system.

The Lagrangian density reads

$$\mathcal{L} = \sum_{j=p,n} \mathcal{L}_j + \mathcal{L}_\sigma + \mathcal{L}_\omega + \mathcal{L}_\rho + \sum_{l=e,\nu} \mathcal{L}_l, \qquad (1)$$

where the nucleon Lagrangian reads

$$\mathcal{L}_j = \overline{\psi}_j \left[\gamma_\mu i D^\mu - M^*\right] \psi_j, \qquad (2)$$

were $M^* = M - g_s\phi$ is the effective baryon mass and

$$iD^\mu = i\partial^\mu - g_v V^\mu - \frac{g_\rho}{2}\tau \cdot \mathbf{b}^\mu. \qquad (3)$$

The meson Lagrangian densities are given by

$$\mathcal{L}_\sigma = \frac{1}{2}\left(\partial_\mu\phi\partial^\mu\phi - m_s^2\phi^2 - \frac{1}{3}\kappa\phi^3 - \frac{1}{12}\lambda\phi^4\right), \qquad (4)$$

$$\mathcal{L}_\omega = \frac{1}{2}\left(-\frac{1}{2}\Omega_{\mu\nu}\Omega^{\mu\nu} + m_v^2 V_\mu V^\mu\right), \qquad (5)$$

$$\mathcal{L}_\rho = \frac{1}{2}\left(-\frac{1}{2}\mathbf{B}_{\mu\nu}\cdot\mathbf{B}^{\mu\nu} + m_\rho^2 \mathbf{b}_\mu\cdot\mathbf{b}^\mu\right), \qquad (6)$$

where $\Omega_{\mu\nu} = \partial_\mu V_\nu - \partial_\nu V_\mu$ and $\mathbf{B}_{\mu\nu} = \partial_\mu \mathbf{b}_\nu - \partial_\nu \mathbf{b}_\mu - g_\rho(\mathbf{b}_\mu \times \mathbf{b}_\nu)$. The lepton Lagrangian densities read

$$\mathcal{L}_l = \overline{\psi}_l \left[\gamma_\mu i\partial^\mu - m_l\right]\psi_l, \qquad (7)$$

where m_e is the electron mass and the neutrino mass is $m_\nu = 0$.

The parameters of the model are three coupling constants g_s, g_v and g_ρ of the mesons to the nucleons, the nucleon mass M, the electron mass m_e, the masses of the mesons m_s, m_v and m_ρ and self-interacting coupling constants κ and λ. The numerical values of the parameters used in this work and usually referred to as NL3 [18] are shown in table I. They are fixed in such a way that the main nuclear matter bulk properties are the binding energy equal to 16.3 MeV at the saturation density 0.148 fm^{-3}, the compressibility is 272 MeV and the effective mass at the saturation density is 0.6 M.

Model	g_s	g_v	g_ρ	M	m_e	m_s	m_v	m_ρ	κ/M	λ
NL3	10.217	12.868	8.948	939.0	0.511	508.194	782.501	763.0	4.377	-173.31

Tabela I. Parameters set used in this work. All masses are given in MeV.

From the Euler-Lagrange formalism we obtain the equations of motion for the nucleons and for the meson fields:

$$\nabla^2\phi = m_s^2\phi + \frac{1}{2}\kappa\phi^2 + \frac{1}{3!}\lambda\phi^3 - g_s\rho_s, \qquad (8)$$

$$\nabla^2 V_0 = m_v^2 V_0 - g_v\rho_B, \qquad (9)$$

$$\nabla^2 b_0 = m_\rho^2 b_0 - \frac{g_\rho}{2}\rho_3, \qquad (10)$$

where ρ_s, ρ_B and ρ_3 are defined next. By replacing the meson fields by their mean values

$$\phi \to \langle\phi\rangle = \phi_0, \qquad (11)$$

$$V_\mu \to \langle V_\mu\rangle = V_0, \qquad (12)$$

$$b_\mu \to \langle b_\mu\rangle = b_0, \qquad (13)$$

the equations of motion read

$$\phi_0 = -\frac{\kappa}{2m_s^2}\phi_0^2 - \frac{\lambda}{6m_s^2}\phi_0^3 + \frac{g_s}{m_s^2}\rho_s, \quad (14)$$

$$V_0 = \frac{g_v}{m_v^2}\rho_B, \quad (15)$$

$$b_0 = \frac{g_\rho}{2m_\rho^2}\rho_3, \quad (16)$$

where $\rho_B = \rho_p + \rho_n$ is the baryonic density and $\rho_3 = \rho_p - \rho_n$, ρ_p and ρ_n are the proton and neutron densities given by

$$\rho_j = 2\int \frac{d^3p}{(2\pi)^3}(f_{j+} - f_{j-}), \quad j = p, n \quad (17)$$

where $f_{j\pm} = 1/(1 + \exp[(\epsilon_j \mp \nu_j)/T])$, $\epsilon_j = \sqrt{p^2 + M^{*2}}$ and $\nu_j = \mu_j - g_v V_0 - g_\rho \tau_3 b_0$, where τ_3 is the appropriate isospin projector for the baryon charge states and μ_j are the nucleon chemical potentials. The scalar density ρ_s is given by

$$\rho_s = 2\sum_{j=p,n}\int \frac{d^3p}{(2\pi)^3}\frac{M^*}{\epsilon_j}(f_{j+} + f_{j-}). \quad (18)$$

The thermodynamic quantities of interest are given in terms of the meson fields. They are the total energy density

$$\mathcal{E}_T = \mathcal{E} + \sum_{l=e,\nu}\mathcal{E}_l, \quad (19)$$

with

$$\mathcal{E} = \frac{1}{\pi^2}\sum_{j=p,n}\int dp\ p^2\sqrt{p^2 + M^{*2}}(f_{j+} + f_{j-}) \quad (20)$$

$$+ \frac{m_v^2}{2}V_0^2 + \frac{m_\rho^2}{2}b_0^2 + \frac{m_s^2}{2}\phi_0^2 \quad (21)$$

$$+ \frac{\kappa}{6}\phi_0^3 + \frac{\lambda}{24}\phi_0^4, \quad (22)$$

the total pressure is

$$P_T = P + \sum_{l=e,\nu}P_l, \quad (23)$$

with

$$P = \frac{1}{3\pi^2}\sum_{j=p,n}\int dp\ p^2\frac{p^4}{\sqrt{p^2 + M^{*2}}}(f_{j+} + f_{j-}) \quad (24)$$

$$+ \frac{m_v^2}{2}V_0^2 + \frac{m_\rho^2}{2}b_0^2 - \frac{m_s^2}{2}\phi_0^2 \quad (25)$$

$$- \frac{\kappa}{6}\phi_0^3 - \frac{\lambda}{24}\phi_0^4, \quad (26)$$

and the total entropy density

$$\mathcal{S} = \frac{1}{T}(\mathcal{E}_T + P_T - \sum_{j=p,n}\mu_j\rho_j - \sum_{l=e,\nu}\mu_l\rho_l), \quad (27)$$

where the electron and electron neutrino energy densities are

$$\mathcal{E}_l = \frac{g_l}{2\pi^2}\int dp\ p^2\sqrt{p^2 + m_l^2}(f_{l+} + f_{l-}), \quad (28)$$

and electron and electron neutrino pressure are

$$P_l = \frac{g_l}{6\pi^2}\int dp\ \frac{p^4}{\sqrt{p^2 + m_l^2}}(f_{l+} + f_{l-}). \quad (29)$$

The electron density ρ_e and electron neutrino density ρ_ν are given by

$$\rho_l = g_l\int \frac{d^3p}{(2\pi)^3}(f_{l+} - f_{l-}), \quad (30)$$

where $g_e = 2$, $g_\nu = 1$, $f_{l\pm} = 1/(1 + \exp[(\epsilon_l \mp \mu_l)/T])$ with $\epsilon_l = \sqrt{p^2 + m_l^2}$ and μ_e is the electron chemical potential, ϵ_ν is the electron neutrino energy and μ_ν is the electron neutrino chemical potential. The condition of β equilibrium in a system of protons, neutrons, electrons and trapped electron neutrinos is

$$\mu_p = \mu_n - \mu_e + \mu_\nu. \quad (31)$$

We impose neutrality of charge as $\rho_p = \rho_e$ and fix the lepton fraction

$$Y_L = \frac{\rho_e + \rho_\nu}{\rho_B}. \quad (32)$$

Notice that muons are not considered in the present calculation.

III. COEXISTING PHASES: NEUTRAL NUCLEAR MATTER WITH NEUTRINO TRAPPING

The formation of pasta phase has been studied lately with great interest [7, 19]. Next we show the main steps for the calculation of the pasta phase with the coexistence phases method based on [20, 21]. For further details, please refer to [11, 13].

For a given total density ρ_B and lepton fraction Y_L we build pasta structures with different geometrical forms in a background nucleon gas with β stability and neutrino trapping. This is achieved by calculating from the Gibbs conditions the density and the particle fractions of the pasta and of the background gas so that in the whole we had to solve simultaneously the following seven equations

$$P^I(\nu_p^I, \nu_n^I, M^{*I}) = P^{II}(\nu_p^{II}, \nu_n^{II}, M^{*II}), \quad (33)$$

$$\mu_n^I = \mu_n^{II}, \quad (34)$$

$$\mu_e^I = \mu_e^{II}, \quad (35)$$

$$\mu_\nu^I = \mu_\nu^{II}, \quad (36)$$

$$m_s^2\phi_0^I + \frac{\kappa}{2}(\phi_0^I)^2 + \frac{\lambda}{6}(\phi_0^I)^3 = g_s\rho_s^I, \quad (37)$$

$$m_s^2\phi_0^{II} + \frac{\kappa}{2}(\phi_0^{II})^2 + \frac{\lambda}{6}(\phi_0^{II})^3 = g_s\rho_s^{II}, \quad (38)$$

$$f(\rho_p^I - \rho_e^I) + (1 - f)(\rho_p^{II} - \rho_e^{II}) = 0, \quad (39)$$

where I and II label each of the phases, f is the volume fraction of phase I

$$f = \frac{\rho_B - \rho^{II}}{\rho^I - \rho^{II}}. \tag{40}$$

The total pressure is given by $P_T = P^I + P_e + P_\nu$. The total energy density of the system is given by

$$\mathcal{E} = f\mathcal{E}^I + (1-f)\mathcal{E}^{II} + \mathcal{E}_e + \mathcal{E}_\nu + \mathcal{E}_{surf} + \mathcal{E}_{Coul}, \tag{41}$$

with $\mathcal{E}_{surf} = 2\mathcal{E}_{Coul}$ [22, 23], and

$$\mathcal{E}_{Coul} = \frac{2\alpha}{4^{2/3}}(e^2\pi\Phi)^{1/3}[\sigma D(\rho_p^I - \rho_p^{II})]^{2/3}, \tag{42}$$

where $\alpha = f$ for droplets, rods and slabs and $\alpha = 1-f$ for bubbles and tubes, σ is the surface energy coefficient, D is the dimension of the system. For droplets, rods and slabs, Φ is given by

$$\Phi = \begin{cases} \left[\left(\frac{2-Df^{1-\frac{D}{2}}}{D-2} + f\right)\frac{1}{D+2}\right], & D = 1, 3, \\ \frac{f-1-\ln(f)}{D+2}, & D = 2, \end{cases} \tag{43}$$

and for bubbles the above expressions are valid with f replaced by $1-f$. The surface tension plays a significant role on the appearance of the pasta phase. In our treatment of the surface tension we essentially follow the prescription given in [11, 13], but some comments on the importance of the surface energy on the calculation of the pasta phase are mandatory. It has been shown that the existence of the pasta phase as the lowest free energy matter and of its internal structures essentially depends on the value of the surface tension [9, 11, 13, 16, 24]. In the present paper the surface energy coefficient is parametrized in terms of the proton fraction according to the functional proposed in [25], obtained by fitting Thomas-Fermi and Hartree-Fock numerical values with a Skyrme force. The same prescription was used in [11, 13]. However, a better recipe is to consider the surface energy coefficient in a consistent way, in terms of relativistic models. In [16] the surface energy was parametrized according to the Thomas-Fermi calculations for three parametrizations of the relativistic NLWM. The Gibbs prescription was used to obtain the σ coefficient which is the appropriate surface tension coefficient to be used [26, 27]. This improvement will be added to our calculations in a forthcoming work.

IV. NEUTRINO CROSS SECTIONS

To calculate neutrino opacities and mean free paths we consider [5] neutral current scattering reactions

$$\nu_e + n \to \nu_e + n, \tag{44}$$
$$\nu_e + p \to \nu_e + p, \tag{45}$$

and charged current absorption reactions

$$\nu_e + n \to e^- + p. \tag{46}$$
$$\overline{\nu}_e + p \to e^+ + n. \tag{47}$$

The cross sections for reactions (44), (45), (46) and (47) employed in this study follow [5]:
Reaction (44):

$$\sigma_n = \begin{cases} \sigma_{ref} = \left(\frac{\sigma_0}{4}\right)\left(\frac{\epsilon_\nu}{m_e c^2}\right)^2, & nND,\ \nu D \text{ or } \nu ND, \\ \sigma_{ref}\left(\frac{\epsilon_\nu}{p_F c}\right)\left(\frac{(1+4g_A^2)}{5}\right), & nD,\ \nu ND,\ [28], \\ \sigma_{ref}\left(\frac{1}{2}\right)\left(\frac{\pi^2(1+2g_A^2)}{8}\right)\times & \\ \left(\frac{T}{\epsilon_\nu}\right)\left(\frac{T}{p_F c}\right)\left(\frac{M^* c^2}{\epsilon_F}\right), & nD,\ \nu D,\ [29, 30]. \end{cases} \tag{48}$$

Reaction (45):

$$\sigma_p = \begin{cases} \sigma_n, & pND,\ \nu D \text{ or } \nu ND, \\ \sigma_n\left(\frac{Y_n}{Y_p}\right)^{1/3}, & pD,\ \nu ND, \\ \sigma_n\left(\frac{Y_n}{Y_p}\right), & pD,\ \nu D,\ [29]. \end{cases} \tag{49}$$

Reactions (46) and (47):

$$\sigma_a = \begin{cases} \sigma_{ref}(1+3g_A^2), & nND,\ \nu ND, \\ \sigma_{ref}(1+3g_A^2)\left(\frac{2Y_p}{Y_n+Y_p}\right), & nND,\ \nu D \text{ or } \nu ND\ [31], \\ \sigma_{ref}(1+3g_A^2)\left(\frac{1}{2}\right)\left(\frac{3\pi^2}{16}\right)\times & \\ \left(\frac{T}{\epsilon_\nu}\right)^2\left(\frac{M^* c^2}{\epsilon_F}\right)\left(\frac{Y_e}{Y_n}\right)^{1/3}, & nD,\ \nu D,\ [28], \\ 0, & nD,\ Y_L < 0.08. \end{cases} \tag{50}$$

In this expressions p_F and ϵ_F mean the Fermi momentum and Fermi energy of the degenerate neutron. Y_e, Y_n, Y_p, Y_L, are the electron, neutron, proton and lepton fractions. ND denotes the non degenerate regime, while D denotes the validity in case of degenerate particles. $\sigma_0 = 1.76 \times 10^{-44}\ cm^2$ and $g_A = 1.254$. Regions of intermediate degeneracy are also handled: the degenerate and non degenerate sectors for both the baryons and the neutrinos of the cross sections detailed in equations (48), (49) and (50) are joined by a simple interpolation algorithm as done in [2]. The total neutrino mean free path in dense matter is given by

$$\lambda_\nu = \frac{1}{\rho_n\sigma_n + \rho_p\sigma_p + \rho_B\sigma_a}. \tag{51}$$

Rosseland neutrino mean free paths are related with diffusion coefficients D_j [4] by

$$\lambda_\nu^k = \frac{D_k}{\int_0^\infty d\epsilon_\nu\ \epsilon_\nu^k f_\nu(1-f_\nu)}, \tag{52}$$

where

$$D_k = \int_0^\infty d\epsilon_\nu\ \epsilon_\nu^k \lambda_\nu f_\nu(1-f_\nu). \quad k = 2, 3, 4 \tag{53}$$

Figura 1. free energy per particle with the NL3 parametrization obtained for $T = 5MeV$ and $Y_L = 0.4$.

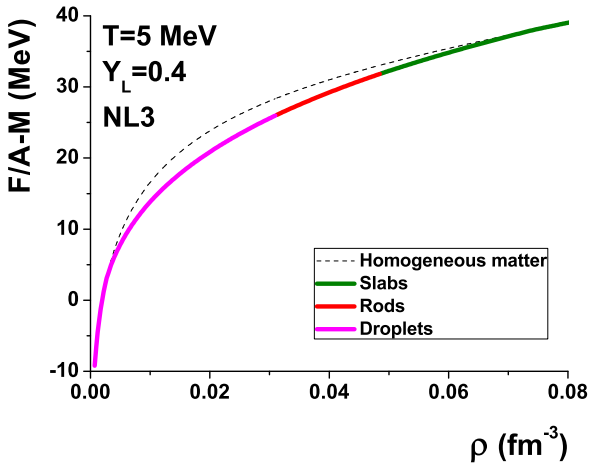

All contributions from neutrino opacities are related with the diffusion coefficients and can to be used as input to the solution of the transport equations in the equilibrium diffusion approximation to simulate the Kelvin-Helmholtz phase of the protoneutron stars [32].

V. RESULTS AND CONCLUSIONS

Before we tackle the problem of the consequences of the pasta phase on the diffusion coefficients, we display a characteristic figure of the free energy for the homogeneous and pastalike matter obtained for $T = 5$ MeV and $Y_L = 0.4$ in Fig. 1. A similar figure is presented in Fig. 9 of [16], but obtained with a relativistic surface energy. One can see that the pasta phase ends when the free energy density reaches the curve for the homogeneous matter. Actually, at this temperature, the pasta phase interpolates between two regions of homogeneous matter, which is the preferential ground state at extremely low densities, as seen in Fig.1. Moreover, the size of the pasta phase decreases with the increase of the temperature and eventually, it no longer exists. It is also worth mentioning that neutrino free matter in β-equilibrium presents a pasta phase smaller than matter with trapped neutrinos [13, 16] as a consequence of the fact that the latter presents a larger fraction of protons. According to studies on binodals and spinodals underlying the conditions for phase coexistence and phase transitions [11, 33, 34], non-homogeneous matter with trapped neutrinos is expected to be found until temperatures around $T = 12$ MeV, depending on the model considered.

We next show the diffusion coefficients D_2, D_3 and D_4 as function of the baryon density for different temperatures obtained for both homogeneous matter and the pasta phase. According to [11, 13] the densities where matter becomes homogeneous depend on the proton fraction and on the temperatures involved, but it is always smaller than 0.1 fm^{-3} for the NL3 parametrization and for the σ values we consider in the present work.

In obtaining the diffusion coefficients, the EoS was calculated as a grid where temperature ranges are in between 0 and 50 MeV and densities vary from 0.005 to 0.5 fm^{-3}. In our codes we have implemented a prescription given in [35] to evaluate the Fermi integrals so that the same codes run from zero (10^{-9}) to high temperatures. We have calculated the diffusion coefficientes only for baryonic densities above 0.005 fm^{-3} because the integrals of type (53) are very difficult to converge at lower densities. We show results for lepton fractions equal to 0.2 and 0.4 because those are typical values necessary in the numerical simulation of protoneutron star evolution.

In all figures the diffusion coefficients obtained with homogeneous matter join the curves obtained with the pasta phase at densities higher than the ones shown. For D_2 calculated at T=5 MeV and $Y_L = 0.4$, for instance, they cross each other at $\rho = 0.12$ fm^{-3}. Our codes interrupt the calculation once homogeneous matter becomes the ground state configuration, as depicted in Fig. 1. This means that there will always be a gap in the diffusion coefficients when the transport equations are calculated with the inclusion of the pasta phase. The same behavior is found at the pressure values for homogeneous and pasta phases at the transition density.

From figures 2, 3 and 4 we can see that only three structures are found inside the pasta phase for the present model: droplets, rods and slabs as far as $Y_L = 0.4$. For $Y_L = 0.2$ only the first two structures remain. While the diffusion coefficients obtained with homogeneous matter is always smooth and continuous, a common trend of all the diffusion coefficients obtained with the pasta phase is a kink at very low densities in between 0.01 and 0.015 fm^{-3}. The interpolation procedure we use depends on the quantities $\eta_i = (\mu_i - M^*)/T, i = p, n$. Whenever either η_p or η_n inverts its sign, these kinks appear, i.e., they are the result of the effective nucleon mass being greater than the corresponding chemical potential. Moreover, the pasta phase diffusion coefficients are always lower than the corresponding coefficients obtained with homogeneous matter.

Our results for the diffusion coefficients D_2 and D_4 are one order of magnitude larger than the results obtained in [32]. This difference can be explained because in the present paper all diffusion coefficients are calculated at very low baryonic densities. For larger densities the results coincide.

In summary we point out that in the present paper we have investigated the influence of the pasta phase on the neutrino opacity by calculating the diffusion coefficients. The homogeneous EoS was obtained with the NL3 parametrization of the NLWM in a mean field approximation. The pasta phase was obtained with the coexistence phases method (CP).

Recent calculations for the pasta phase within the Thomas-Fermi approximation at finite temperatures [36]

show that the internal pasta structure is much richer as compared with the CP method we have employed in the present work. Hence, the dependence on the structure of the pasta phase is also of interest and this calculation is planned for different parametrizations of the NLWM. More sophisticated matter, which includes the α-particles should also be considered [16].

We have checked that the neutrino interactions in warm and low baryonic densities with pasta formation show significant differences when compared with homogeneous matter. Next the temporal evolution of the PNS will be calculated and, in face of the present results, we expect that the cooling and deleptonization eras will be influenced by the presence of the pasta phase at low densities.

An obvious improvement is the inclusion of hyperons in the EoS. However, the pasta phase can still be computed just with protons, neutrons and light clusters because hyperons are expected to appear only at densities where the pasta phase is no longer present.

ACKNOWLEDGMENTS

This work was partially supported by the Brazilian sponsoring bodies CNPq and CAPES (M.D. Alloy scholarship).

[1] J. M. Lattimer and M. Prakash, Science **304**, 536 (2004).
[2] W. Keil and H. Janka, Astron. Astrophys. **296**, 145 (1995).
[3] J.A. Pons, A.W. Steiner, M. Prakash and J.M. Lattimer, Phys.Rev.Lett. **86** (2001) 5223-5226.
[4] J.A. Pons, S. Reddy, M. Prakash, J.M. Lattimer and J.A. Miralles, Astrophys. J. 513, 780 (1999).
[5] A. Burrows and J. M. Lattimer, Astrophs. J 307, 178 (1986).
[6] D. Ravenhall, C.J. Pethick and J.R. Wilson, Phys. Rev. Lett. **50**, 2066 (1983).
[7] C. J. Horowitz, M. A. Perez-Garcia, and J. Piekarewicz, Phys. Rev. C **69**, 045804 (2004).
[8] C.J. Horowitz, M.A. Pérez-Garcia, D.K. Berry and J. Piekarewicz, Phys. Rev. **C 72**, 035801 (2006).
[9] T. Maruyama, T. Tatsumi, D.N. Voskresensky, T. Tanigawa and S. Chiba, Phys. Rev. **C 72**, 015802 (2005).
[10] G. Watanabe and H. Sonoda, cond-mat / 0502515
[11] S.S. Avancini, D.P. Menezes, M.D. Alloy, J.R. Marinelli, M.M.W. de Moraes and C. Providência, Phys. Rev. **C 78**, 015802 (2008).
[12] J. Xu, L.W. Chen, B.A. Li and H.R. Ma, arXiv:0807.4477v1 [nucl-th].
[13] S.S. Avancini, L. Brito, J.R. Marinelli, D.P. Menezes, M.M.W. de Moraes, C. Providência and A.M. Santos - Phys. Rev. **C 79**, 035804 (2009).
[14] H. Sonoda, G. Watanabe, K. Sato, T. Takiwaki, K. Yasuoka, T. Ebisuzaki, Phys. Rev. C 75, 042801 (2007).
[15] G. Watanabe, H. Sonoda, T. Maruyama, K. Sato, K. Yasuoka, T. Ebisuzaki, Phys. Rev. Lett. 103, 121101 (2009).
[16] S.S. Avancini, C.C. Barros, D.P. Menezes and C. Providência, Phys. Rev. C 82, 025808 (2010).
[17] B. Serot and J.D. Walecka, *Advances in Nuclear Physics* 16, Plenum-Press, (1986) 1.
[18] G. A. Lalazissis, J. König and P. Ring, Phys. Rev. **C 55**, 540 (1997).
[19] G. Watanabe et al., Physical Review Letters **94**, 031101 (2005).
[20] , M. Barranco and J. R. Buchler, Phys. Rev. C 22, 1729 (1980).
[21] D. P. Menezes and C. Providência, Phys. Rev. C 60, 024313 (1999).
[22] , D. G. Ravenhall, C. J. Pethick and J. R. Wilson,Phys. Rev. Lett 50, 2066 (1983).
[23] T. Maruyama, T. Tatsumi, D. N. Voskresensky, T. Tanigawa and S. Chiba, Phys. Rev. C 72, 015802 (2005).
[24] G. Watanabe, K. Iida and K. Sato, Nucl. Phys. A676, 455 (2000); G. Watanabe, K. Iida and K. Sato, Nucl. Phys. A687, 512 (2001); G. Watanabe, K. Iida and K. Sato, Nucl. Phys. A726, 357 (2003).
[25] J.M. Lattimer, C.J. Pethick, D.G. Ravenhall, D.Q. Lamb, Nucl. Phys. **A432**, 646 (1985).
[26] M. Centelles, M. Del Estal and X. Viñas, Nucl. Phys. **A 635**, 193 (1998).
[27] W. D. Mayers and W. J. Swiatecki, Phys. Rev. C **63**, 034318 (2001).
[28] N. Iwamoto, Ph.D. thesis, AA(Illinois Univ., Urbana-Champaign.), 1981.
[29] B. T. Goodwin and C. J. Pethick, Astrophys. J.**253**, 816 (1982).
[30] R. F. Sawyer and A. Soni, Astrophys. J.**230**, 859 (1979).
[31] S. A. Bludman and K. A. van Riper, Astrophys. J.**224**, 631 (1978).
[32] S. Reddy, M. Prakash and J.M. Lattimer, Phys. Rev. **D 58**, 013009 (1998).
[33] C. Ducoin, C. Providência, A. M. Santos, L. Brito and Ph. Chomaz, Phys. Rev. **C 78**, 055801 (2008).
[34] H. Pais, A. Santos and C. Providência, Phys. Rev. C **80**, 045808 (2009).
[35] J.M. Aparicio, Astrophys. J. Suppl. 117 (1998) 627.
[36] S.S. Avancini, S. Chiacchiera, D.P. Menezes and C. Providência, arXiv:1010.3644v1 [nucl-th].

Figura 2. Diffusion coefficient D_2 as function of baryon density for different temperature and proton fraction values for homogeneous matter and pasta phase.

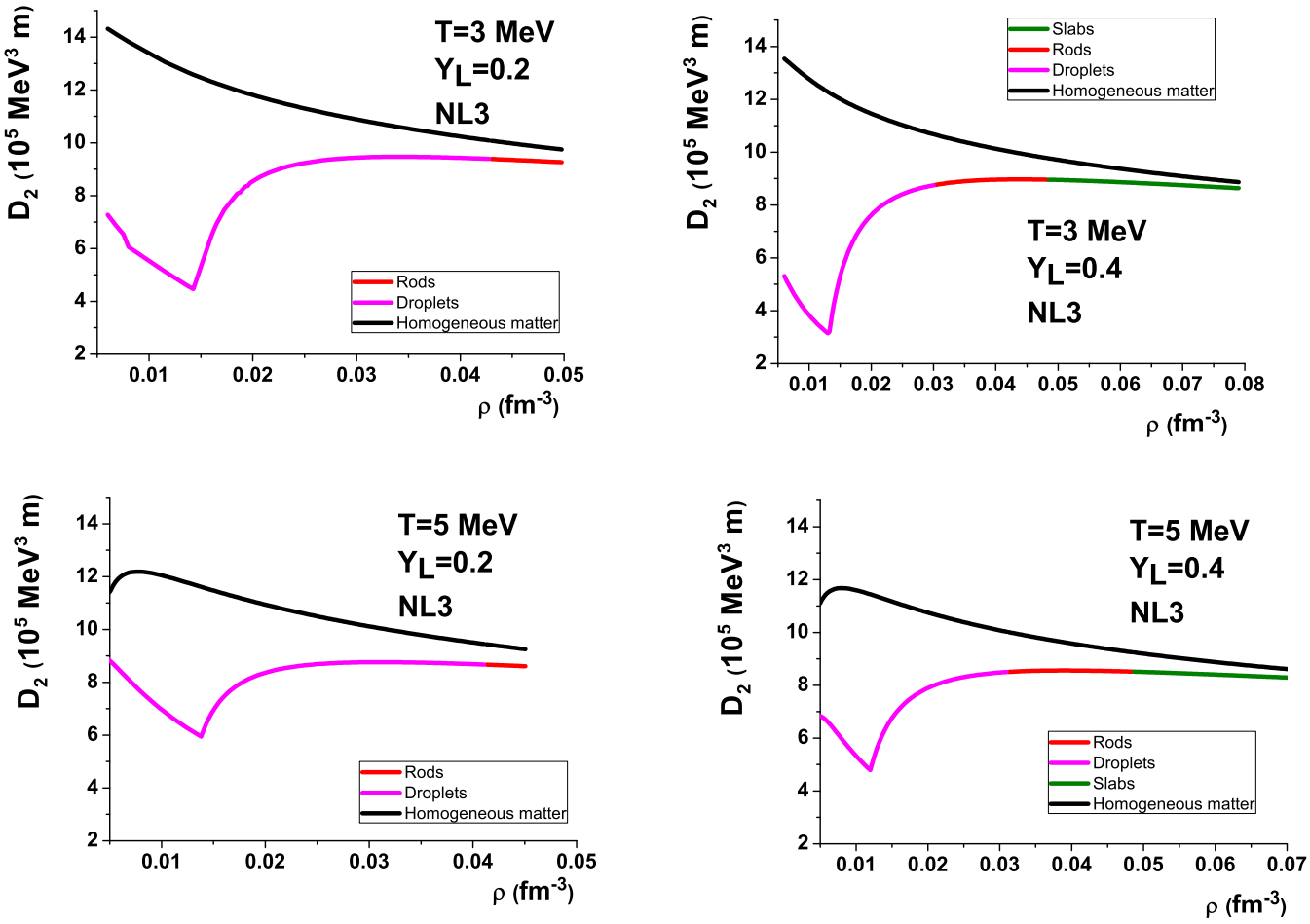

Figura 3. Diffusion coefficient D_3 as function of baryon density for different temperature and proton fraction values for homogeneous matter and pasta phase.

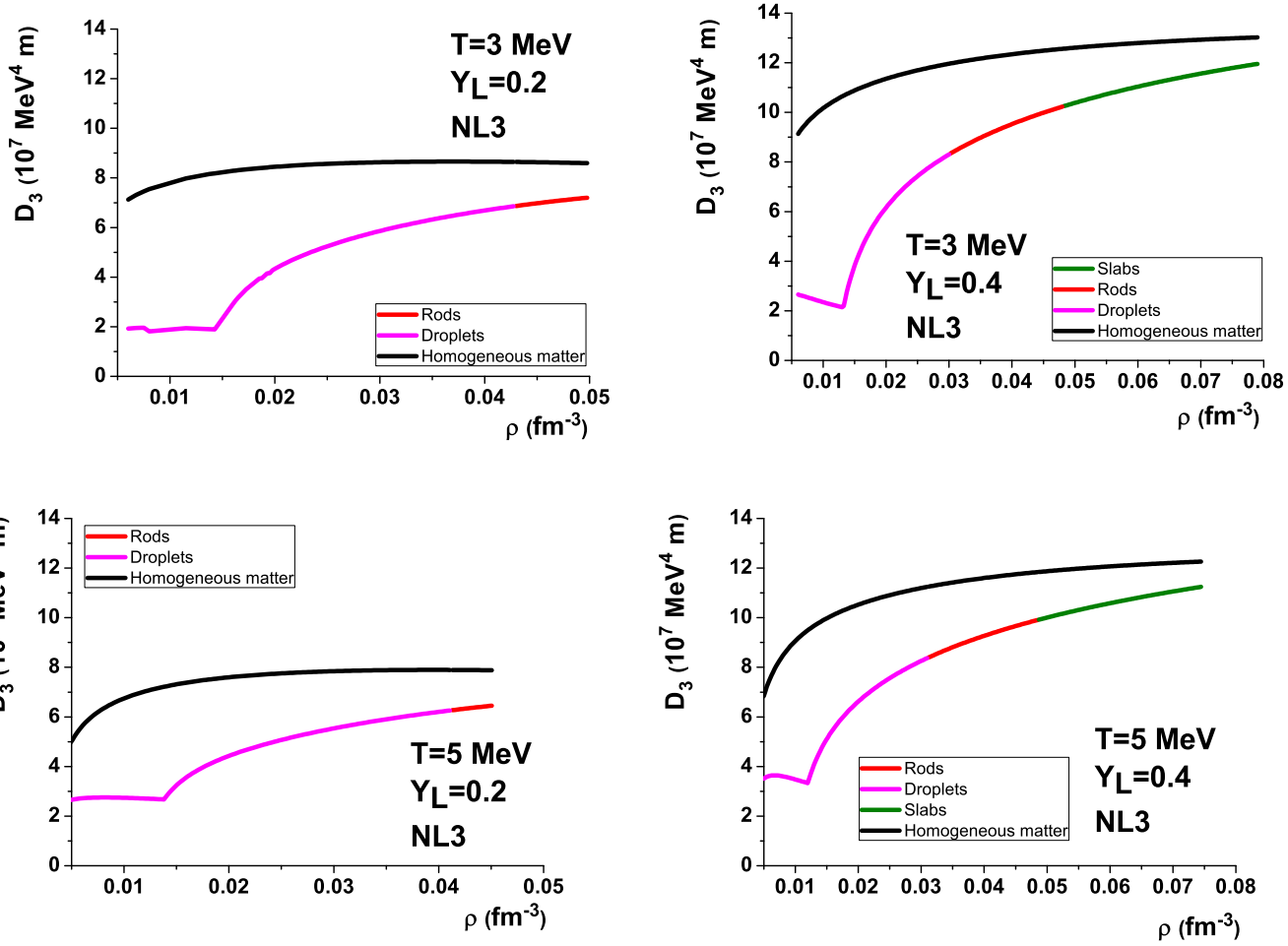

Figura 4. Diffusion coefficient D_4 as function of baryon density for different temperature and proton fraction values for homogeneous matter and pasta phase.